Description of pairing correlation in many-body finite systems with density functional theory

Guillaume Hupin and Denis Lacroix
Grand Accélérateur National d'Ions Lourds (GANIL), CEA/DSM-CNRS/IN2P3, Bvd Henri Becquerel, 14076 Caen, France
(Received 20 October 2010; published 28 February 2011)

Different steps leading to the new functional for pairing based on natural orbitals and occupancies proposed earlier [D. Lacroix and G. Hupin, Phys. Rev. B **82**, 144509 (2010)] are carefully analyzed. Properties of quasiparticle states projected onto good particle numbers are first reviewed. These properties are used to (i) prove the existence of such a functional, (ii) provide an explicit functional through a $1/N$ expansion starting from the BCS approach, and (iii) give a compact form of the functional summing up all orders in the expansion. The functional is benchmarked in the case of the picket-fence pairing Hamiltonian where even and odd systems are studied, using the blocking technique, at various particle numbers and coupling strengths, with uniform and random single-particle level spacing. In all cases, very good agreement is found, with a deviation of $<1\%$ compared to the exact energy.

DOI: 10.1103/PhysRevC.83.024317 PACS number(s): 21.60.Jz, 74.20.Fg

I. INTRODUCTION

Nuclear systems [1,2] or ultrasmall metallic grains [3] offer the possibility of obtaining insight into the finite pairing correlations of systems with varying particle number. The introduction of a simple many-body wave packet ansatz more than 50 years ago by Bardeen, Cooper, and Schrieffer (BCS) [4] was a major breakthrough for the understanding and description of superconductivity. To illustrate the advantages and drawbacks of the BCS theory, in Fig. 1, the condensation energy, i.e., the difference between the Hartree-Fock (HF) energy and the energy of the system obtained with BCS (dashed line) is compared to the exact result (solid line) for the picket-fence pairing Hamiltonian (for details, see Sec. IV) [5–7]. One of the great advantages of the BCS or Hartree-Fock Bogoliubov (HFB) theory is the possibility, at the price of conserving only the average particle number, of grasping part of the correlation beyond the Hartree-Fock level while keeping the theory relatively simple. As can be seen from Fig. 1, the BCS prediction becomes closer to the expected result as the number of particles increases. Indeed, the BCS theory is shown to be exact in the thermodynamic limit. Besides these interesting aspects, BCS or HFB suffer from a threshold at low coupling. In fact, when the coupling strength is much smaller than the average level spacing between single-particle states, BCS identifies with HF, while, in reality, correlations build up as soon as the two-body interaction is plugged in. In addition, even above the threshold, parts of the correlation are systematically missed.

It is now standard practice to use BCS or HFB theories in nuclear physics, for instance, within the energy density functional (EDF) approach [8,9] leading to the so-called single-reference (SR-EDF) or mean-field level of EDF. These tools already provide a rather good reproduction of gross nuclear properties. For instance, masses can be estimated with a typical precision of 500–600 keV. Figure 1, however, clearly points out that there is room for improving the BCS approach in finite size systems. In particular, part of the discrepancy stems from the use of a trial wave function that is not an eigenstate of the particle number operator $\hat{N}$. Starting from the BCS wave packet, a new state with a good particle number can be obtained using the projection operator technique [10]. Within EDF, similar to the restoration of angular momentum or calculation including dynamical fluctuations associated with configuration mixing, projection onto a good particle number enters into the class of multireference EDF (MR-EDF). If the projection is made prior to the variation [variation after projection (VAP)], the variational state directly becomes an eigenstate of $\hat{N}$. Illustration of VAP condensation energy (open circles) is given in Fig. 1 (see, for instance, Ref. [11]). Such an approach provides a very accurate description of pairing correlation at all coupling strengths and completely removes the BCS threshold problem. VAP still remains rather involved numerically, and a less efficient but simpler approach consists of projecting the state after the variation, the so-called projection after variation (PAV) (open triangles in Fig. 1). The projection technique is becoming a popular tool in nuclear structure. However, recent studies have shown that projection aiming at restoring broken symmetries and/or more generally configuration mixing should be handled with care when combined with density functional theory [12,13], due to the possible appearance of jumps and/or divergences in the energy surface. These difficulties have been carefully analyzed in Refs. [14–16] and have been related to the self-interaction and self-pairing problem. By comparing theories starting from a Hamiltonian and an energy functional, a correction to the pathologies was proposed such that systematic calculation along the nuclear chart is now within reach. These studies have clearly pointed out that specific aspects might appear due to the use of functional theories (see also Refs. [17,18]) when MR-EDF is used.

The EDF framework provides a unified framework not only for nuclear structure but also for nuclear dynamics and thermodynamics. While MR-EDF is a suitable tool for the former, due to its complexity, it can hardly be used in the latter cases. The goal of the present work is to discuss a new approach to treat pairing where the projection effect is directly incorporated into the functional through specific dependencies on natural orbital occupancies. Such an approach, directly

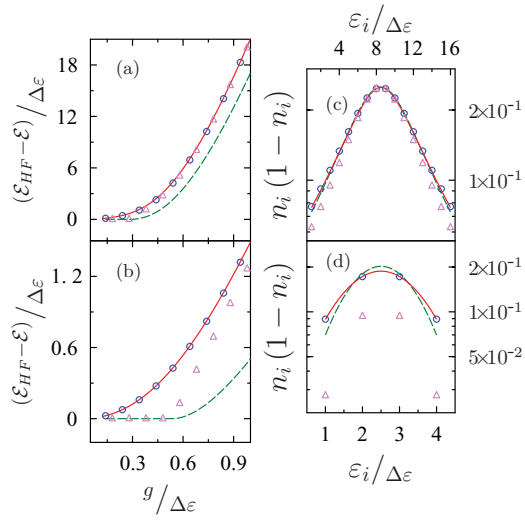

FIG. 1. (Color online) Exact condensation energy (red solid line) obtained for the picket-fence pairing Hamiltonian as a function of the coupling strength for 16 (top) and 8 (bottom) particles. In both cases, the BCS (green dashed line) and the projected BCS with a projection made before (open blue circle) or after the variation (open violet triangle) are also shown. On the right, occupation numbers of the different theories are plotted for $g/\Delta\varepsilon = 0.82$.

written in the functional framework, avoids some ambiguities encountered in current EDF and is expected to greatly simplify PAV and to be easily adapted to the nonequilibrium evolution of finite temperature studies. The main aspects of the new functional theory have already been summarized in Ref. [19]. Here, we present a complete discussion of the different steps leading to the functional. Below, we first discuss the interest of using natural orbital based functionals. Then, mathematical properties of projected BCS states that are used to propose the functional are given. Finally, the new functional is applied to a specific pairing Hamiltonian either with equidistant or nonequidistant level spacing and benchmarked for any coupling strength and particle number.

II. FUNCTIONALS BASED ON NATURAL ORBITALS AND OCCUPANCIES

The possibility of replacing a many-body problem by a functional of the density matrix was first proposed by Gilbert [20] and is called density matrix functional theory (DMFT) or reduced DMFT (RDMFT). The Gilbert theorem is a generalization of the Hohenberg-Kohn theorem [21] where the variational quantity, i.e., the local density $\rho(\mathbf{r}, \mathbf{r})$, is replaced by the full one-body density matrix (OBDM) $\rho(\mathbf{r}, \mathbf{r}')$. Most often, the OBDM is first written in the natural or canonical basis as $\rho = \sum_i |\varphi_i\rangle n_i \langle\varphi_i|$. Here n_i and $\{|\varphi_i\rangle\}$ denote occupation numbers and natural orbitals, respectively. Then, the initial many-body problem is replaced by the minimization of an energy functional

$$\mathcal{F}[\{\varphi_i\},\{n_i\}] = \mathcal{E}[\{\varphi_i\},\{n_i\}] - \mu\{\mathrm{Tr}(\hat{N}\rho) - N\} - \sum_{ij}\lambda_{ij}(\langle\varphi_i|\varphi_j\rangle - \delta_{ij}), \quad (1)$$

where the variation is made with respect to both single-particle states $\varphi_i^*(\mathbf{r})$ and occupation numbers. The set of Lagrange multipliers μ and $\{\lambda_{ij}\}$ are introduced to ensure particle number conservation and orthogonality of the single-particle states. RDMFT has several advantages compared to the standard density functional theory (DFT). For instance, while Kohn-Sham single-particle states used to construct the local density are not expected to have physical meaning, the nonlocal density ρ should match the exact one at the minimum. Accordingly, associated single-particle states and occupations identify with those of the exact many-body state. This is an important aspect of this theory. Indeed, DFT can only provide information on the energy. In RDMFT, not only the energy can be estimated but also any one-body operators. Similary to density functional theory, the main challenge is to find accurate functionals.

Another interesting feature of this theory is its ability to describe aspects that are not adequately obtained at the DFT level, such as reactions, atomization energy, or the dissociation of small molecules. All these phenomena have their counterparts in nuclear physics. Nowadays, a sizable effort is made to provide new accurate RDMFT functionals and benchmark them on finite and infinite systems (see, for instance, Ref. [22] and references therein).

In this article, we focus on pairing. Let us first remark that current SR-EDFs that account for pairing already share many aspects with RDMFT. Most nuclear SR-EDFs used now start from a functional that can be written as

$$\begin{aligned}\mathcal{E}_{\mathrm{SR}}[\rho, C] &\equiv \mathcal{E}^{\rho} + \mathcal{E}^{\rho\rho} + \mathcal{E}^{C} \\ &= \sum_{ij} t_{ij}\,\rho_{ji} + \frac{1}{2}\sum_{ijkl}\bar{v}^{\rho\rho}_{ijkl}\,\rho_{ki}\,\rho_{lj} \\ &\quad + \frac{1}{4}\sum_{ijkl}\bar{v}^{C}_{klij}\,C_{ij,kl},\end{aligned} \quad (2)$$

where $\bar{v}^{\rho\rho}$ and $\bar{v}^{C}$ denote effective two-body kernels, respectively, in the particle-hole and correlation channels. $C_{1,2}$ denotes the irreducible two-body correlation matrix defined as the difference between the two-body density and the antisymmetric product of a one-body density matrix (see, for instance, Ref. [23]). To treat pairing correlations, a quasiparticle trial state $|\phi_{\mathrm{QP}}\rangle$ is considered, then the correlation matrix elements can be written in terms of the anomalous density κ as $C_{ij,kl} = \kappa^*_{ij}\kappa_{kl}$ [1,14]. In the natural orbital basis, the quasiparticle state can be expressed in a BCS form,

$$|\phi_{\mathrm{QP}}\rangle = \prod_i (1 + x_i a_i^\dagger a_{\bar{i}}^\dagger)|0\rangle, \quad (3)$$

where $|0\rangle$ corresponds to the particle vacuum, while $\{a_i^\dagger, a_{\bar{i}}^\dagger\}$ correspond to doubly degenerated canonical states $\{\varphi_i, \varphi_{\bar{i}}\}$ with occupation probability $2n_i$. The x_i coefficients are connected to the occupation numbers through

$$|x_i|^2 = \frac{n_i}{(1-n_i)}. \quad (4)$$

Accordingly, pairing energy reduces to

$$\mathcal{E}^C = \frac{1}{4}\sum_{ij}\bar{v}^{\kappa\kappa}_{i\bar{i}j\bar{j}}\sqrt{n_i(1-n_i)}\sqrt{n_j(1-n_j)}.$$

Noting in addition that both $\mathcal{E}^\rho$ and $\mathcal{E}^{\rho\rho}$ can directly be written as a functional of n_i and φ_i through their dependence on the one-body density, we see that current SR-EDF can indeed be interpreted as a mapping between the initial problem into a functional theory of $(\{\varphi_i\}, \{n_i\})$, i.e.,

$$\mathcal{E}[\rho, C] \rightarrow \mathcal{E}[\{\varphi_i\}, \{n_i\}], \tag{5}$$

provided that the functional is written in the canonical basis. EDF based on quasiparticle states have the shortcomings discussed in the Introduction when combined with projection onto a good particle number within the MR-EDF. This is nowadays used in nuclear structure study. If the projection is made prior to the variation, such a projection is equivalent to considering a new trial wave function, called hereafter generically the projected BCS (PBCS) state, of the form

$$|N\rangle \equiv \hat{P}^N|\phi_{\rm QP}\rangle \propto \left(\sum_i x_i a_i^\dagger a_{\bar{i}}^\dagger\right)^N |0\rangle, \tag{6}$$

where $\hat{P}^N$ is the projector on particle number N (see, for instance, Refs. [10,13,16]). In the following, we will use the short notation $\Gamma^\dagger = \sum_i x_i b_i^\dagger$ with $b_i^\dagger = a_i^\dagger a_{\bar{i}}^\dagger$.

When projection is made in a EDF, the associated functional becomes much more complex to minimize. It should, however, be noted that the functional is generally written in terms of the normal and anomalous density of the original quasiparticle state from which the projected state is constructed. Therefore, the occupation probabilities of the new trial state $|N\rangle$ do not appear directly [24]. Nevertheless, the occupation numbers of $|N\rangle$ can be estimated numerically. Illustration of occupation probabilities of the projected states are compared to the exact ones for the picket-fence pairing Hamiltonian in Fig. 1. Both VAP and PAV results as well as BCS case are displayed. It is first interesting to mention that, while the energy is improved in the PAV case, single-particle occupation numbers deviate more from the exact solution than in the original BCS case. This is something to worry about since, when PAV is performed in EDF, expectation values of one-body operators are estimated. In contrast, in the VAP method, occupation probabilities perfectly match the exact case for all particle numbers and pairing coupling strengths. Therefore, we see that the use of the projected state before the variation leads to a very good reproduction of both the ground state energy and the single-particle occupation numbers.

Having this in mind, in the following, we use the properties of the PBCS state to provide a new functional for pairing directly based on the occupation numbers of the projected state. The state (6) is used as a starting point where it is implicitly assumed that the orbitals are written in their canonical basis, namely, the one which exhibits an explicit time-reversal symmetry. In that case, the energy (2) reduces to[1]

$$\mathcal{E}_{\rm SR}[\rho^N, C^N] = \sum_i t_i\, n_i^N + \frac{1}{2}\sum_{ij}\bar{v}^{\rho\rho}_{iijj}\,\rho^N_{ii}\,\rho^N_{jj} + \frac{1}{4}\sum_{ij}\bar{v}^{C}_{i\bar{i}j\bar{j}}\,C^N_{i\bar{i},j\bar{j}}, \tag{7}$$

were $\rho^N_{ii} = n_i^N$ and $C^N_{i\bar{i},j\bar{j}}$ now stand for the occupation and correlations associated with the projected state, i.e.,

$$n_i^N = \frac{\langle N|a_i^\dagger a_i|N\rangle}{\langle N|N\rangle}, \quad C^N_{ij} = \frac{\langle N|b_i^\dagger b_j|N\rangle}{\langle N|N\rangle} - \delta_{ij}n_i^N n_j^N. \tag{8}$$

Here, we have used the compact notation $C^N_{ij} \equiv C^N_{i\bar{i},j\bar{j}}$. In the following, we will omit the N label to shorten the notation, keeping in mind that these quantities refer to the projected state. In order to do the mapping (5), we are left with the challenge of expressing the correlation C_{ij} as a functional of n_i as it can be easily done in the BCS or HFB case. But in the present work, we aim at accounting for the particle number conservation directly in the functional.

III. CONSTRUCTION OF FUNCTIONALS FOR PAIRING FROM A PBCS STATE

Here, some properties of projected states are first highlighted. These properties are then used as guidance in constructing the functional. Over the years, interesting features of matrix elements entering in Eq. (8) have been derived. Some can eventually be deduced using the fact that the BCS state plays the role of the PBCS state generating function [25,26] and can be used, for instance, to minimize the energy directly written as a functional of the $\{x_i\}$ parameters [27,28]. Proofs of some of the properties that are used below are first given.

A. Definition of a class of operators, states, and overlaps

First, we start with a strategy similar to that in Ref. [29]. A set of pair creation operators that omit one, two, . . . pairs of single-particle states is first introduced:

$$\begin{aligned}\Gamma^\dagger(i) &= \Gamma^\dagger - x_i b_i^\dagger,\\ \Gamma^\dagger(i,j) &= \Gamma^\dagger - x_i b_i^\dagger - x_j b_j^\dagger,\\ &\cdots\end{aligned} \tag{9}$$

where indices i, j refer to the removed pairs. In the following, Ω will denote the size of the single-particle Hilbert space. From these operators, a corresponding set of states with a

[1]Note that, correlation matrix elements should also appear in the particle-hole channel. Since the aim of the present article is to focus on the pairing channel and since these components cancel out exactly in the example presented below, they are omitted here.

given particle number is defined:

$$\begin{aligned} |K\rangle &= c_K(\Gamma^\dagger)^K|-\rangle, \\ |K:i\rangle &= c_K(\Gamma^\dagger(i))^K|-\rangle, \\ |K:i,j\rangle &= c_K(\Gamma^\dagger(i,j))^K|-\rangle, \\ &\cdots \end{aligned} \tag{10}$$

with $K \leqslant N$, while c_K is taken by convention equal to $(K!)^{-1/2}$. Note that the state introduced in Eq. (6) corresponds to the special situation where $K = N$ and no pair has been removed. From these states, we define a set of coefficients from the overlaps:

$$\begin{aligned} I_K &= K!\langle K|K\rangle \\ I_K(i) &= K!\langle K:i|K:i\rangle \\ I_K(i,j) &= K!\langle K:i,j|K:i,j\rangle \\ &\cdots \end{aligned} \tag{11}$$

Using the fact that $(b_j^\dagger)^2 = 0$, due to the fermionic nature of the particles, the different operators verify that

$$\begin{aligned} [\Gamma^\dagger(i_1,\ldots,i_\kappa)]^K = [\Gamma^\dagger(i_1,\ldots,i_\kappa,j)]^K \\ + K x_j [\Gamma^\dagger(i_1,\ldots,i_\kappa,j)]^{K-1}. \end{aligned} \tag{12}$$

This property leads to specific relationships between the states defined above and their overlaps. For instance,

$$\begin{aligned} I_K &= I_K(i) + K|x_i|^2 I_{K-1}(i), \\ I_K(i) &= I_K(i,j) + K|x_j|^2 I_{K-1}(i,j), \\ &\cdots \end{aligned} \tag{13}$$

These recurrence relations have been recently used to solve numerically VAP [27] and will be at the heart of the present work to design a new functional for pairing.

B. Energy as an explicit functional of $\{x_i\}$

Since the PBCS state is written as a functional of the parameter set $\{x_i\}$, expectation values of any operators can *a priori* be expressed as a functional of this set. Here, an illustration is given for the occupation probabilities and correlation matrix elements.

Using the states defined in Eq. (10), the expectation values of operators entering into Eq. (8) can be expressed as

$$\begin{aligned} \langle N|a_i^\dagger a_i|N\rangle &= |x_i|^2\langle N-1:i|N-1:i\rangle, \\ \langle N|b_i^\dagger b_j|N\rangle &= x_i^* x_j\langle N-1:i|N-1:j\rangle. \end{aligned} \tag{14}$$

We then deduce that both occupation numbers and correlation components can be expressed in terms of ratios between the different coefficients introduced in Eqs. (11):

$$\begin{aligned} n_i &= N|x_i|^2\frac{I_{N-1}(i)}{I_N}, \\ C_{ij} &= N x_i^* x_j \frac{I_{N-1}(i,j)}{I_N} \quad \text{for} \quad (i \neq j), \end{aligned} \tag{15}$$

while for $i = j$, $C_{ii} = n_i(1-n_i)$. Overlaps entering in n_i and C_{ij} can be directly expressed as a functional of $\{x_i\}$. Indeed, a direct development of $(\Gamma^\dagger)^K$ in Eq. (6) gives

$$\begin{aligned} |N\rangle &= c_K \sum_{(i_1,\ldots,i_N)}^{\neq} x_{i_1}\cdots x_{i_N} b_{i_1}^\dagger \cdots b_{i_N}^\dagger|-\rangle, \\ &= K!c_K \sum_{i_1<\cdots<i_K\leqslant\Omega}^{\neq} x_{i_1}\cdots x_{i_N} b_{i_1}^\dagger \cdots b_{i_N}^\dagger|-\rangle, \end{aligned}$$

where $\sum_{(i_1,\ldots,i_N)}^{\neq}$ is used to insist that the summation is made only for indices different from each other. From this expression, it is straightforward to see that

$$I_K = \sum_{(i_1,\ldots,i_K)}^{\neq} |x_{i_1}|^2\cdots|x_{i_K}|^2. \tag{16}$$

In a similar way, the following expressions can be deduced:

$$\begin{aligned} I_K(i) &= \sum_{(i_1,\ldots,i_K)\neq i}^{\neq} |x_{i_1}|^2\cdots|x_{i_K}|^2, \\ I_K(i,j) &= \sum_{(i_1,\ldots,i_K)\neq(i,j)}^{\neq} |x_{i_1}|^2\cdots|x_{i_K}|^2, \\ &\cdots \end{aligned}$$

Note that, these expressions also suggest additional sum rules between the overlap:

$$\begin{aligned} I_K &= \sum_i |x_i|^2 I_K(i), \\ I_K(i) &= \sum_{j\neq i} |x_j|^2 I_K(i,j), \\ &\cdots \end{aligned} \tag{17}$$

For completeness, additional properties are given in Appendix A. Reporting the above expressions into Eq. (15), both n_i and C_{ij}, and consequently the energy, take the form of an explicit functional of $\{x_i\}$. This functional turns out to be too complex for direct practical use unless one can take advantage of the different recurrence relation to estimate the desired quantities [27].

C. Energy as an implicit functional of $\{n_i\}$

The possibility of writing the energy as a functional of natural orbitals and occupation probabilities is far from being trivial. Strictly speaking, the Gilbert theorem [20] holds for systems bound by an external potential. It could, however, be extended to self-bound systems with the introduction of the Legendre multiplier technique [30]. In practice, such a technique is useful when the energy can first be written as a functional of the single-particle energies through some preliminary approximations (see, for instance, Refs. [31,32]). In general, the existence of an occupation number functional as well as its form is not straightforward. Here, we give a proof of the principle that the energy estimated with a PBCS trial wave can indeed be written as such a functional. Since all quantities can be written as a functional of $\{x_i\}$, it is sufficient

to prove that these parameters can in turn be put as a function of the $\{n_i\}$ set.

Starting from the expression of n_i and taking advantage of Eq. (17), we first obtain

$$n_i = N \sum_{j\neq i} |x_i|^2 |x_j|^2 \frac{I_{N-2}(i,j)}{I_N}. \tag{18}$$

Then, using the following recurrence relations

$$I_{N-1}(i) = I_{N-1}(i,j) + (N-1)|x_j|^2 I_{N-2}(i,j),$$
$$I_{N-1}(j) = I_{N-1}(i,j) + (N-1)|x_i|^2 I_{N-2}(i,j),$$

which are valid for any $i \neq j$, we see that

$$I_{N-1}(i,j) = \frac{|x_j|^2 I_{N-1}(j) - |x_i|^2 I_{N-1}(i)}{|x_j|^2 - |x_i|^2},$$
$$I_{N-2}(i,j) = \frac{1}{N-1} \frac{I_{N-1}(i) - I_{N-1}(j)}{|x_j|^2 - |x_i|^2}, \tag{19}$$

from which we deduce

$$n_i(N-1) = \sum_{j\neq i} |x_i|^2 |x_j|^2 \frac{|x_j|^2 n_i - |x_i|^2 n_j}{|x_j|^2 - |x_i|^2}. \tag{20}$$

Eventually, it can be transformed as

$$N(1-n_i) = \sum_{j\neq i} (n_j - n_i) \frac{|x_j|^2}{|x_j|^2 - |x_i|^2}. \tag{21}$$

This expression holds for any single-particle state i. This set of coupled equations between occupation numbers and $\{x_i\}$ is of particular interest for the present discussion. Indeed, given a set of occupation numbers n_i, one could *a priori* deduce the values of the x_i through these secular equations. This shows that these parameters are an implicit functional of the occupation probabilities (see also discussion in Sec. IV).

D. Energy as an explicit functional of $\{n_i\}$

In this section, we discuss the main objective of the present work, i.e., to provide an explicit functional of the occupation probabilities. The strategy that is followed here is to use the BCS case as a guidance (see Appendix B). In that case, there is a direct and simple relation between $|x_i|^2$ and n_i already given in Eq. (4). Let us first see how this relation can be generalized in the PBCS case.

Using the first equation of Eq. (13) for $K = N$ and reporting in the denominator appearing in n_i leads to

$$n_i = \frac{|x_i|^2}{|x_i|^2 + \alpha_N(i)}, \tag{22}$$

where we have introduced the notation $\alpha_N(i) \equiv I_N(i)/[N I_{N-1}(i)]$. This expression can easily be inverted and compared to Eq. (4). In the PBCS case, we have

$$|x_i|^2 = \left(\frac{n_i}{1-n_i}\right) \alpha_N(i). \tag{23}$$

Therefore, we see that the BCS limit is recovered if $\alpha_N(i) = 1$ and that all the physics beyond the ordinary BCS or HFB theories is contained in its deviation from unity. This could also be seen by expressing the correlation in terms of n_i and $\alpha_N(i)$. Reporting Eq. (19) into (15) leads to

$$C_{ij} = \begin{cases} n_i(1-n_i) & \text{for} \quad (i=j), \\ x_i^* x_j \frac{n_j - n_i}{|x_j|^2 - |x_i|^2} & \text{for} \quad (i \neq j). \end{cases} \tag{24}$$

Taking advantage of Eq. (23) and using the short-hand notation $\alpha_i \equiv \alpha_N(i)$ finally gives (for $i \neq j$)

$$C_{ij} = \sqrt{n_i(1-n_i) n_j (1-n_j) \alpha_i \alpha_j} \times \frac{n_i - n_j}{n_i(1-n_j)\alpha_i - n_j(1-n_i)\alpha_j}. \tag{25}$$

In the limit $\alpha_i = 1$, the BCS functional $C_{ij} = \sqrt{n_i(1-n_i) n_j (1-n_j)}$ is recovered. More generally, it is shown that any of the following quantities, defined through

$$\alpha_K(i_1, \ldots, i_\kappa) = \frac{1}{K} \frac{I_K(i_1, \ldots, i_\kappa)}{I_{K-1}(i_1, \ldots, i_\kappa)}, \tag{26}$$

identify with 1 in the BCS limit (see Appendix B).

1. $1/N$ expansion beyond the BCS theory

Since the BCS theory identifies with PBCS in the large N limit, it is reasonable to seek for a correction to $\alpha_K(i_1, \ldots, i_\kappa) = 1$ written as a $1/N$ expansion. Such an expansion can be obtained thanks to the relation

$$\alpha_K(i_1, \ldots, i_K) = \frac{1}{K} \sum_{j\neq(i_1,\ldots,i_K)}^{\neq} |x_j|^2 \frac{\alpha_{K-1}(i_1, \ldots, i_K, j)}{|x_j|^2 + \alpha_{K-1}(i_1, \ldots, i_K, j)}, \tag{27}$$

connecting α_K and α_{K-1} terms. This expression can be derived using Eqs. (13) and (17). Due to the presence of a $1/K$ prefactor in this relation, any correction of order $1/(K-1)$ in α_{K-1} will appear as an order $1/K(K-1)$ in α_K. As an illustration, assuming that $\alpha_{N-1}(i,j) \simeq 1$, as in BCS, leads to

$$\alpha_N(i) \simeq \frac{1}{N} \sum_j \frac{|x_j|^2}{|x_j|^2 + 1} \simeq \frac{1}{N} \sum_j n_j = \frac{1}{N}(N - n_i) = 1 - \frac{1}{N} n_i, \tag{28}$$

which appears as the first-order correction in $(1/N)$ to the BCS case. Similarly, we can obtain

$$\alpha_{N-1}(i,j) \simeq \frac{1}{N-1}(N - n_i - n_j)$$
$$\alpha_{N-2}(i,j) \simeq \frac{1}{N-2}(N - n_i - n_j - n_k)$$
$$\ldots$$

Higher order corrections in $\alpha_N(i)$ can be obtained by including more and more terms in the expansion of all α_K (with $K < N$). This technique has been used in Ref. [19] to get the expansion

$$\alpha_N(i) = 1 - \frac{1}{N} n_i + \frac{1}{N(N-1)} \sum_{j\neq i} n_j^2 [1 - (n_i + n_j)]$$

$$+\frac{1}{N(N-1)(N-2)}\sum_{(k,j)\neq i}^{\neq} \times n_j^2 n_k^2[2-(n_i+n_j+n_k)]+\cdots, \tag{29}$$

which corresponds to $\alpha_N(i)$ written as an explicit functional of the occupation numbers. Note that additional terms tested numerically as negligible and appearing at the second (or higher) order approximation are omitted here. This functional can then be injected into Eq. (25), leading to an explicit functional of x_i in terms of the n_i. Accordingly, expectation values of any operator becomes also a functional of the projected state occupation numbers.

This approximation was tested numerically in Ref. [19] and showed a rapid convergence in the strong coupling limit. However, for small coupling (HF limit), a slow convergence was found. Indeed, assuming that $n_i \to 1$ for the N pairs, we deduce for one of the occupied state

$$\sum_{j\neq i} n_j^2[1-(n_i+n_j)] \to -(N-1),$$

$$\sum_{(k,j)\neq i}^{\neq} n_j^2 n_k^2[2-(n_i+n_j+n_k)] \to -(N-1)(N-2),$$

$$\cdots$$

Therefore, in this limit, all contributions to any order will participate to the same extent and sum to give $\alpha_N(i) = (1-n_i)$, leading finally to a correlation given by

$$C_{ij} \to \sqrt{n_i n_j}. \tag{30}$$

This form, which has been proposed using a completely different strategy in an electronic system [33], will never be properly described by the BCS functional. From the discussion above, difficulties in the application of the present functional might also be anticipated. Indeed, since all terms in the expansion should be kept, the functional becomes rather complicated and its application might become rapidly intractable.

2. *Resummation of the* $1/N$ *expansion and simplified functional*

The price to pay to correctly describe the weak coupling limit is to keep all orders in the expansion presented above. This basically shows that the $1/N$ expansion approach starting from the BCS approximation is not appropriate in that case. To overcome this difficulty a simplified functional can be found using the following approximation in Eq. (29):

$$\frac{1}{N(N-1)}\sum_{j\neq i} \to \frac{1}{N^2}\sum_j,$$

$$\frac{1}{N(N-1)(N-2)}\sum_{(k,j)\neq i}^{\neq} \to \frac{1}{N^3}\sum_{jk}\cdots,$$

while keeping all terms in this expansion. This approximation leads to a simple linear dependence of the α_i coefficient with respect to the occupation numbers n_i:

$$\alpha_i = a_0 - a_1 n_i, \tag{31}$$

where a_0 and a_1 are given by the expressions

$$a_1 = \frac{1}{N}\left(1+s_2+s_2^2+\cdots+s_2^{N-1}\right) = \frac{1}{N}\frac{1-s_2^N}{1-s_2} \tag{32}$$

and

$$a_0 = 1+\frac{(s_2-s_3)}{N}\left[1+2s_2+\cdots+(N-1)s_2^{N-2}\right] = 1+(s_2-s_3)\frac{\partial a_1}{\partial s_2}, \tag{33}$$

and where the moments $s_p = \frac{1}{N}\sum_i (n_i)^p$ have been used. Reporting expression (31) in the correlation matrix elements of Eq. (25) gives the simple form (for $i \neq j$)

$$C_{ij} = \sqrt{n_i(1-n_i)n_j(1-n_j)} \times \frac{\sqrt{(a_0-a_1 n_i)(a_0-a_1 n_j)}}{a_0-a_1(n_i+n_j-n_i n_j)}, = \mathcal{C}(n_i,n_j). \tag{34}$$

The functional (34) together with Eqs. (32) and (33) represent the main result of this article. We can already anticipate some advantages of this functional. (i) In the Hartree-Fock limit $s_p = 1$ for all $p > 1$. Accordingly, $a_0 = a_1 = 1$ and we recover the HF functional quoted above, i.e., $C_{ij} = \sqrt{n_i n_j}$. (ii) The BCS limit is also easily identified in Eq. (34) by taking the limit $a_0 = 1$ and $a_1 = 0$. The net result of our approach is that the energy introduced in Eq. (7) that was originally written as a functional of the density and correlations in the projected state becomes now a functional of the one-body density matrix components only. In practice, such a functional approach should be solved by minimizing Eq. (1) where the energy now reads

$$\mathcal{E}_{\rm SR}[\{\varphi_i\},\{n_i\}] = \sum_i t_i\, n_i + \frac{1}{2}\sum_{ij}\bar{v}^{\rho\rho}_{iijj}\, n_i n_j + \frac{1}{4}\sum_{i\neq j}\bar{v}^{C}_{i\bar{i}j\bar{j}}\,\mathcal{C}(n_i,n_j) + \frac{1}{4}\sum_i \bar{v}^{C}_{i\bar{i}i\bar{i}}\, n_i(1-n_i).$$

First applications of this functional can be found in Ref. [19], illustrating the predicting power of the functional for energy and occupation probabilities. In numerical implementation, sequential quadratic programming leads to very good convergence at any coupling and/or large particle number. Below, the new functional is further illustrated and benchmarked.

IV. APPLICATION

We consider here a system of A particles interacting through the pairing Hamiltonian of the form [5–7]

$$H = \sum_{i>0}\varepsilon_i(a_i^\dagger a_i + a_{\bar{i}}^\dagger a_{\bar{i}}) - \frac{g}{2}\sum_{i,j} a_i^\dagger a_{\bar{i}}^\dagger a_{\bar{j}} a_j, \tag{35}$$

where $\bar{i}$ denotes the time-reversed state of i, both associated with single-particle energy ε_i. The total single-particle Hilbert space size is assumed to be $\Omega = 2A$. This Hamiltonian can be solved exactly numerically by making use of the so-called Richardson equations. The first test of the functional was made with this model Hamiltonian for an even particle number $A = 2N$, where N denotes the number of pairs, and for equidistant single-particle levels, the so-called picket-fence Hamiltonian. Here, we will further illustrate some of the aspects of the new functional in that case, and extend the application to even systems ($A = 2N + 1$) and/or nonequidistant levels.

A. Illustration in the picket-fence Hamiltonian

Here, we first consider the special case of equidistant single-particle levels with a level spacing denoted by $\Delta\varepsilon$. First, we recall that the strategy to design a functional going beyond the BCS one was made in three steps: (i) The parameters $\{x_i\}$ were first shown to be implicit functional of the $\{n_i\}$ through the existence of a set of secular equations [Eq. (21)]. (ii) Starting from the BCS prescription, systematic $1/N$ corrections were proposed to obtain a new functional [Eq. (29)]. (iii) Summing all orders, a simplified functional was then introduced [Eq. (31)]. Step (ii) has been shown to be inadequate [19], especially in the weak coupling limit. In the following, we further illustrate the gain in predicting power of the form (34) compared to the original BCS prescription.

1. *Application of the new functional for equidistant level spacing*

We first consider the case of even systems with doubly degenerated equidistant levels. In the following, the condensation energy, denoted by $\mathcal{E}_{\rm Cond}$, is defined as

$$\mathcal{E}_{\rm Cond} = \mathcal{E}_{\rm HF} - \mathcal{E}, \tag{36}$$

where $\mathcal{E}_{\rm HF} = 2\sum_{i>0}\varepsilon_i - gN$ is the Hartree-Fock (HF) energy while $\mathcal{E}$ denotes the energy of the considered theory. $\mathcal{E}_{\rm Cond}$ quantifies the predicting power of different approximations. An illustration of the evolution of this quantity as a function of the coupling strength has already been given in the Introduction (Fig. 1). In Fig. 2, we see that the proposed functional is almost on top of the exact result (and the exact VAP calculation). A slight difference is observed in the intermediate coupling regime. Similarly, occupation numbers perfectly match the exact ones in the strong coupling regime and slightly differ from them below the BCS threshold. In this regime, while BCS identifies with HF, here, occupation probabilities different from 1 and 0 are obtained as soon as the interaction is switched on.

2. *Critical discussion of the linear approximation, Eq. (31)*

Figure 3 shows the accuracy of the present approximation in the model case of a constant two-body interaction g. In this figure, the approximate α_i for different coupling strength $g/\Delta\varepsilon = 0.32$ (filled circles), 0.64 (crosses), and 0.96 (open circles) are compared to the exact ones (respectively, dashed, dotted, and solid lines) as a function of either the orbital probabilities [Fig. 3(a)] or single-particle energies [Fig. 3(b)]

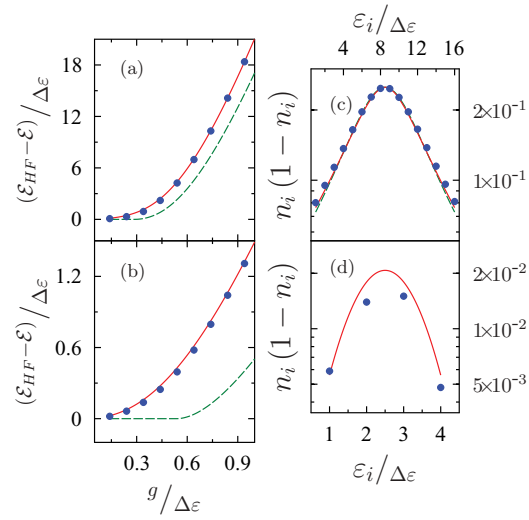

FIG. 2. (Color online) Evolution of the condensation energy for the exact (red solid line), BCS (green dashed line), and new functional (blue filled circles) obtained for the picket-fence pairing Hamiltonian as a function of the coupling strength for (a) 16 and (b) 8 particles. On the right, occupation numbers of the different theories are plotted for (c) $g/\Delta\varepsilon = 0.82$ and (d) $g/\Delta\varepsilon = 0.22$.

at the minimum of energy. The dependency of α_i obtained in the PBCS case for small coupling also shows that a simple linear approximation cannot fully grasp the physics of weak coupling. Following the same strategy as above, quadratic or cubic corrections might eventually be obtained. However, this will add complexity to the functional while the energy is already rather well reproduced.

3. *Systematic analysis of occupation numbers*

In Fig. 2, illustrations of occupation numbers obtained in different theories are shown for specific couplings. In a DMFT framework, not only the energy should match the exact energy at the minimum but also the deduced one-body density matrix, and *a fortiori* occupation numbers should also be identical to the exact one. To systematically compare the gain in predicting single-particle occupation numbers in the new functional, we

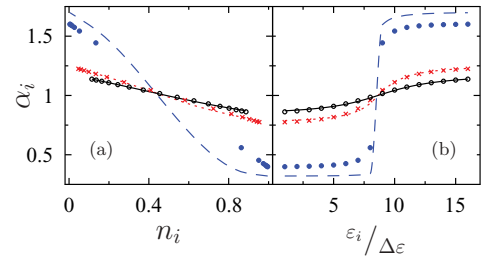

FIG. 3. (Color online) Evolution of the coefficients α_i as a function of n_i (a) or ε_i (b) at the minimum of energy. The different curves correspond to the PBCS result for $g/\Delta\varepsilon = 0.32$ (dashed line), 0.64 (dotted line), and 0.96 (solid line). The corresponding results obtained with the linear approximation [Eq. (31)] are displayed by filled circles, crosses, and open circles, respectively.

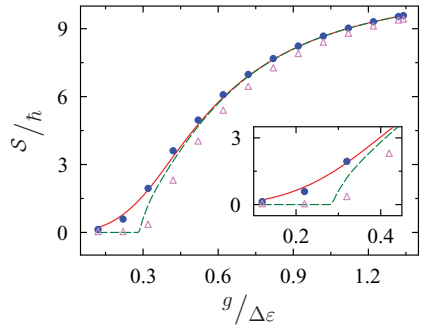

FIG. 4. (Color online) Evolution of the one-body entropy for different theories as a function of the coupling strength for 16 particles. The BCS (green dashed line), PAV (open violet triangles), and PBCS-functional (filled blue circles) ansatz are compared to the exact result. The inset magnifies the low $g/\Delta\varepsilon$ vicinity.

have defined the one-body entropy:

$$\mathcal{S}[n_i] = -\sum_i [n_i \ln(n_i) + (1-n_i)\ln(1-n_i)]. \tag{37}$$

The entropy evolution is shown in Fig. 4 as a function of the coupling strength. While PAV and BCS are unable to reproduce the exact result, especially below or in the vicinity of the threshold, the new functional is in close agreement with it.

4. Simplified functional for the strong coupling regime

One important issue from the practical point of view is the possibility to further simplify in some regime. In particular, in the strong coupling regime, we have seen that $1/N$ perturbation starting from BCS rapidly converges to the exact solution. Truncation at second order of Eq. (29) already gives a very good result [19]. It is therefore legitimate to question whether a simpler form for Eq. (34) can be found in this regime. Close to BCS, we expect $a_0 \to 1$ and $a_1 \to 0$ which justifies an expansion in orders of (a_1/a_0). For instance,

$$C_{ij} = \sqrt{n_i n_j (1-n_i)(1-n_j)} \times \left[1 - \frac{a_1}{2a_0}[n_i(1-n_j) + n_j(1-n_i)] + O\left(\frac{a_1}{a_0}\right)\right].$$

In Fig. 5, leading order (LO) and next to next to leading order (N^2LO) are compared as a function of the pairing strength for a typical number of particles, $A = 16$, from 0 and 1 to the exact distribution. It can be inferred that the full functional solution can only be recovered at low coupling strength when all terms of the expansion are taken into account, which agrees with the previous discussion leading to resummation.

5. Application to odd systems

Similar to the BCS framework, the energy of systems with an odd number of particles can be obtained by using blocking techniques. In the PBCS case, this is equivalent to considering a modified trial wave function given by

$$|2N+1\rangle \propto (a_\alpha^\dagger + a_{\bar{\alpha}}^\dagger)[\Gamma^\dagger(\alpha)]^N|-\rangle, \tag{38}$$

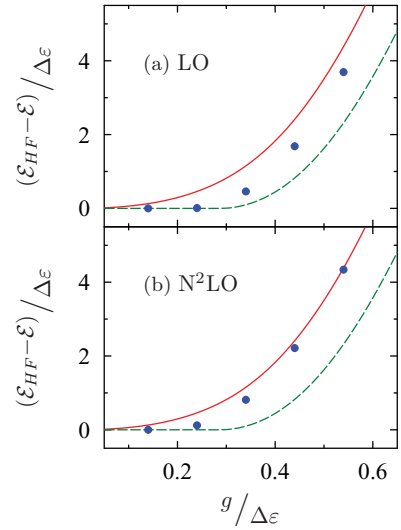

FIG. 5. (Color online) Comparison between leading order (a) and next to next to leading order (b) of the new functional (blue filled circles) for 16 particles. Evolution of the condensation energy for the exact (red solid line) and BCS (green dashed line) are shown as references.

which does preserve the time-reversal symmetry of the solution. Here, $\{\alpha, \bar{\alpha}\}$ correspond to the blocked pair and identify with the last occupied levels in the Hartree-Fock limit. The particle number conservation implies that occupation of the blocked states are kept fixed and equal to $n_b = n_{\bar{b}} = 0.5$. As an illustration of the odd-even effect, we define the average gap $\bar{\Delta}$ through the relation

$$\bar{\Delta} = \frac{\mathcal{E}_C}{\sum_{i\neq b}\sqrt{n_i(1-n_i)}}. \tag{39}$$

This quantity identifies up to a factor $1/g$ with the standard gap in the BCS limit. In Fig. 6, the evolution of $\bar{\Delta}/A$ as a function of particle number A is presented for different values of the coupling strength in the exact (solid line), BCS (dashed line), and new functional (filled circles) cases. Odd particle numbers (left column) are compared with even ones (right) to distinguish the odd-even effect. This figure shows that the new functional predicts well $\bar{\Delta}/A$ for both even and odd number of particles. Deviations at low coupling strength of the PBCS from the exact case stem from the small discrepancies in the occupation numbers between those obtained in the functional formulation and the exact ones. The insets of Fig. 6 show the standard deviations from the exact calculation normalized to unity for the different functionals. It is worth mentioning that the same accuracy is observed for both even and odd systems in the case of the PBCS functional, this is in contrast with the BCS calculations. In the following discussion, the effect of particle number is further investigated.

6. Accuracy of the functional with respect of particle number

It is known from Ref. [34] that the PBCS state exhibits slight deviations from the exact solution for medium number of particles. Since our approach is based on a PBCS trial

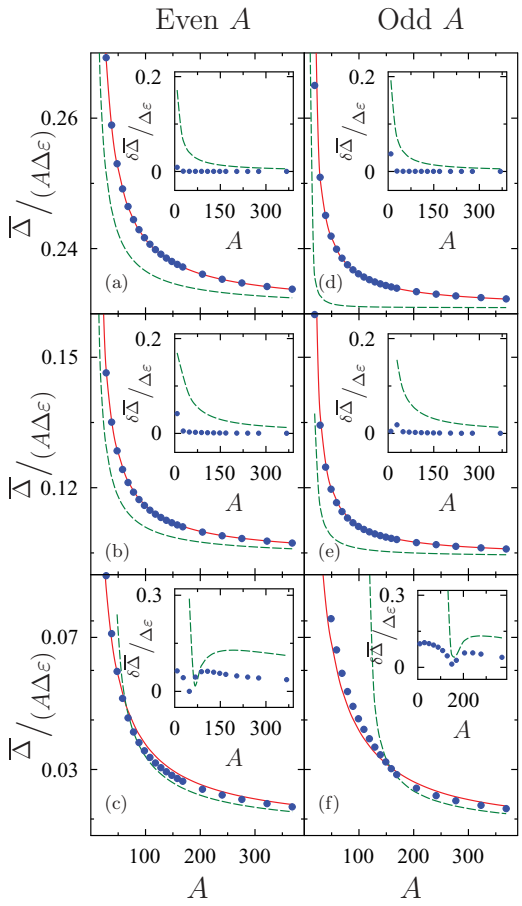

FIG. 6. (Color online) Evolution of $\bar{\Delta}/A$ as a function of particle number A for even (left) and odd (right) systems. From top to bottom, the three different coupling constants $g/\Delta\varepsilon = 0.66$, 0.44, and 0.224 are shown. In each case, the BCS (green dashed line) and PBCS (blue filled circles) functional theories are compared to the exact calculation (red solid line). Note that $g/\Delta\varepsilon = 0.224$ is below the BCS threshold for some values A which leads to an equivalent threshold in the quantity $\bar{\Delta}/A$. In the insets, the standard deviations to the exact calculation renormalized to 1 are compared for the different functionals.

state, we do expect a similar behavior. To systematically address the quality of the PBCS functional with respect to both the number of nucleons and the coupling strength, the condensation energies for odd and even systems are displayed in Fig. 7 as a function of $d/\widetilde{\Delta}$ [34], where

$$d/\widetilde{\Delta} \equiv \frac{2}{A}\sinh(1/g)$$

for $g/\Delta\varepsilon = 0.224$ [Fig. 7(a)] and $g/\Delta\varepsilon = 0.44$ [Fig. 7(b)]. In this figure, particle numbers ranging from $A = 8$ (large d) to $A = 360$ (small d) have been used. This figure illustrates the improvement of the new functional compared to BCS. It also clearly shows that some deviations from the exact results persist in the new functional. It should, however, be kept in mind that the observed deviations correspond to less than 1% of errors in the total energy. This is illustrated in the insets of

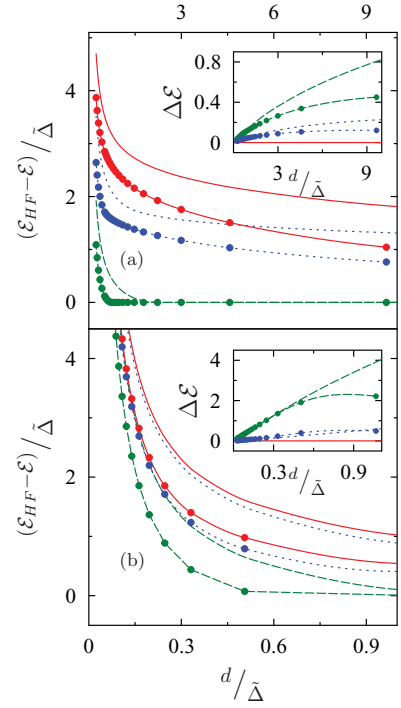

FIG. 7. (Color online) Condensation energy predicted by the BCS functional (green dashed line) and the PBCS functional (blue filled circles) compared to the exact solution (red solid line) for varying $d/\widetilde{\Delta}$ and for $g/\Delta\varepsilon = 0.224$ (a) and $g/\Delta\varepsilon = 0.44$ (b). In each case, curves corresponding to even and odd particle numbers are shown, the latter being displayed with additional filled circles. In the insets, relative error (in percent) on the total energy with respect to the exact solution made in the BCS and PBCS functionals is shown.

Fig. 7, where the relative error defined as

$$\Delta\mathcal{E} = 100\frac{\mathcal{E} - \mathcal{E}_{\text{exact}}}{\mathcal{E}_{\text{exact}}},$$

where $\mathcal{E}_{\text{exact}}$ is the exact energy, is displayed as a function of $d/\widetilde{\Delta}$. As expected, error tends to zero in all cases as A increases ($d \to 0$). For intermediate to high coupling [Fig. 7(b)], a good agreement between the PBCS based functional and the exact solution is obtained, while at lower coupling strength some deviations appear. This results both from the approximation scheme used to design the functional (linear approximation for the α_i, see Ref. [19]) and from the accuracy of PBCS theory itself as an approximation of the exact trial wave function. It should indeed be kept in mind that the present functional is entirely based on the PBCS theory which already deviates from the exact solution (see, for instance, Refs. [35,36]). As a consequence, it could only lead to results which are at most equivalent to the PBCS approximation. From the comparison between Fig. 7(a) and Ref. [37], it can be inferred that deviations at low g stem from (i) the deviation of the PBCS result from the exact solution as A increases and (ii) the additional approximations made to obtain the functional that lead to an increase of the deviation compared to PBCS as $A \to 0$. Nevertheless, we see from this comparison that the PBCS based functional is much more competitive than the

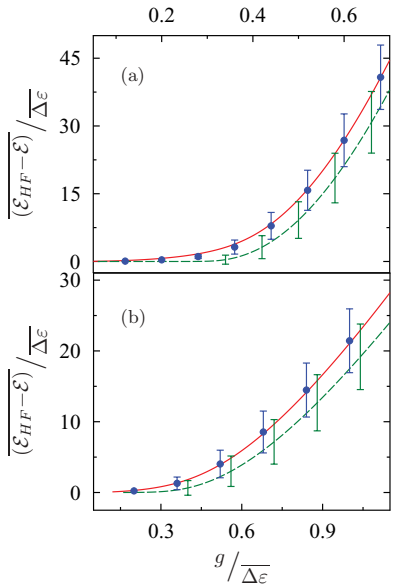

FIG. 8. (Color online) Evolution of the average condensation energy and its statistical fluctuation (displayed by error bars) as a function of $g/\overline{\Delta\varepsilon}$ for the PBCS based functional (blue filled circles), the BCS functional (green dotted line) for $A = 41$ (a) $A = 16$ (b). The exact solution (red solid line) for an equidistant level spacing $\Delta\varepsilon_i$ of unit is shown as reference.

BCS theory and is expected to be much easier to implement than PBCS itself.

B. Application to randomly spaced levels

As a final illustration of the functional theory application, we consider here a set of randomly spaced levels. Following Refs. [37,38], an ensemble of random spectrum is generated by the central eigenvalues of a $2A \times 2A$ random matrix. Thus, the set of energy levels belongs to the Gaussian orthogonal ensemble, see Ref. [39]. The renormalization proposed in Ref. [38] is performed, where

$$\varepsilon \to 1/2\pi[4A \sin^{-1}(\varepsilon/\sqrt{4A}) - \varepsilon\sqrt{4A-\varepsilon^2}], \qquad (40)$$

so that the average level energy spacing is of the order of unity. As an illustration, the evolution of average condensation energy and its statistical fluctuation as a function of $g/\overline{\Delta\varepsilon}$ are shown in Fig. 8 obtained with the PBCS functional (filled circle) and the BCS functional (dotted line). Again and as expected, the new functional matches the reference result of the exact solution for an equidistant level spacing $\Delta\varepsilon = 1$. This last application illustrates that the method can be applied to systems with various level densities.

V. CONCLUSION

In this work, quasiparticle states projected onto good particle numbers are used as a starting point to propose new functionals dedicated to pairing correlations. The properties of projected states are first reviewed. These properties are then used to get a functional of occupation numbers and natural orbitals of the trial wave function. The new functional is benchmarked with the pairing Hamiltonian either with equidistant or with randomly distributed single-particle energies for even and odd systems. In all cases, a very good agreement with the exact result is obtained, showing great improvement over the BCS theory. Origins of the remaining deviations are discussed.

The possibility of using a new functional that accounts for particle number conservation opens new perspectives for the study of mesoscopic systems where pairing plays an important role. One may, for instance, anticipate new applications for thermodynamics or dynamics where direct projection are too complex to provide a practical tool. In addition, this might also be a tool of choice for avoiding recent difficulties encountered in nuclear structure studies (see, for instance, Ref. [14]).

The application to the picket fence shows that our approach might be suitable to incorporate both pairing and particle number projection in a functional approach. It should, however, be noted that the present framework gives a specific role to the canonical basis. Indeed, the functional form only holds in this basis. Therefore, the use of our method implies the need to develop codes for realistic application in this basis, which is at variance with respect to most of the standard methods used presently to perform particle number restoration and might lead to practical difficulties. While the present application clearly shows that the method is successful for rather general single-particle energy spectra or rather large particle numbers, the search for and use of a canonical basis in up-to-date realistic applications of an energy density functional to nuclei is a much more difficult task. In particular, new aspects emerge such as the necessity to treat correlations not only in the particle-particle or hole-hole channel but also in the particle-hole channel or the strategy to be followed to use density-dependent effective interactions. It turns out that we recently made important progress in addressing these questions and applied density matrix functional theory to nuclei showing that the present approach might be a valuable tool for nuclei. An extensive discussion of the application to realistic nuclei including practical aspects related to the use of a canonical basis will be given elsewhere [40].

ACKNOWLEDGMENTS

We are particularly grateful to N. Sandulescu for providing us the exact Richardson and PBCS codes. We also thank Th. Duguet for helpful discussions.

APPENDIX A: FURTHER PROPERTIES OF I_K, $I_K(i)$, ...

In this appendix, properties of the overlaps defined in Eqs. (11) are further developed. The discussion below is especially useful to make the connection with recent works and between PBCS and BCS states. Using expression (17) for I_K and taking advantage of the recurrence relation (13) gives

$$I_K = \sum_i |x_i|^2 I_{K-1} - (N-1)\sum_i |x_i|^4 I_{K-2}(i).$$

In a similar way, $I_{K-2}(i)$ can be expressed in terms of I_{K-2} through

$$I_{K-2}(i) = I_{K-2} - (K-2)|x_i|^2 I_{K-3}(i),$$

leading to

$$I_K = \sum_i |x_i|^2 I_{K-1} - (K-1)\sum_i |x_i|^4 I_{K-2} + \cdots$$

Iterating this procedure K times leads to

$$I_K = \sum_{n=1}^{K} (-1)^{n+1} \frac{(K-1)!}{(K-n)!} I_{K-n} X_n, \tag{A1}$$

where only overlaps I_L (with $L < K$) appear in the right-hand side and where the coefficients

$$X_n \equiv \sum_j |x_j|^{2n}$$

are introduced. According to the above expression (A1), any I_K can be written in a determinant form as

$$I_K = \begin{vmatrix} X_1 & 1 & 0 & 0 & \cdots & 0 \\ X_2 & X_1 & 2 & 0 & \cdots & 0 \\ X_3 & X_2 & X_1 & 3 & \cdots & 0 \\ & & \cdots & & & \\ X_{K-1} & X_{K-2} & X_{K-3} & X_{K-4} & \cdots & (K-1) \\ X_K & X_{K-1} & X_{K-2} & X_{K-3} & \cdots & X_1 \end{vmatrix}. \tag{A2}$$

The same expression was obtained by Rowe [25,26] using a completely different starting point, making connection with the elementary symmetric Schur polynomial. Besides this expression, similar to transformation between elementary symmetric polynomials and power sums X_K, it is worth mentioning that other relations exist linking other bases of the symmetric polynomial algebra [41].

The same procedure can also be followed for the different quantities $I_K(i)$, $I_K(i,j), \ldots$, leading to a form similar to Eq. (A2) where the X_n have been respectively replaced by $X_n(i)$, $X_n(i,j), \ldots$, with

$$X_n(i) \equiv \sum_{j\neq i} |x_j|^{2n},$$
$$X_n(i,j) \equiv \sum_{k\neq(i,j)} |x_j|^{2n},$$
$$\cdots$$

APPENDIX B: GUIDANCE FROM THE BCS THEORY

The BCS or HFB framework has played an important role in developing the new functional proposed in this work. We give here highlights of some aspects discussed in the text. Let us start with a state given by Eq. (3). To connect with the PBCS notation, we write

$$|N\rangle \equiv \prod_k (1 + x_k b_k^\dagger)|-\rangle, \tag{B1}$$

keeping in mind that, in the quasiparticle many-body case, the particle number N is only conserved in average and has only a meaning in the thermodynamics limit. In analogy with the PBCS case, we introduce the set of states $|N-1:i\rangle$ such that

$$\langle N|N\rangle = \langle N:i|N:i\rangle + |x_i|^2\langle N-1:i|N-1:i\rangle,$$
$$\langle N|a_i^\dagger a_i|N\rangle = |x_i|^2\langle N-1:i|N-1:i\rangle,$$
$$\langle N|b_i^\dagger b_j|N\rangle = x_i^* x_j\langle N-1:i|N-1:j\rangle.$$

Starting from Eq. (B1), we directly see that states verifying the above relations also verify

$$|N:i\rangle = |N-1:i\rangle = \cdots = \prod_{k\neq i}(1 + x_k b_k^\dagger)|-\rangle.$$

Using similar analogies between relations that hold in both PBCS and BCS cases, we can also deduce

$$|N:i,j\rangle = |N-1:i,j\rangle = \cdots = \prod_{k\neq(i,j)} (1 + x_k b_k^\dagger)|-\rangle, \tag{B2}$$
$$\cdots$$

Noting that the coefficient α_K introduced in the text also verify

$$\alpha_K(i) = \frac{\langle K:i|K:i\rangle}{\langle K-1:i|K-1:i\rangle},$$
$$\alpha_K(i,j) = \frac{\langle K:i,j|K:i,j\rangle}{\langle K-1:i,j|K-1:i,j\rangle}, \tag{B3}$$
$$\cdots$$

We directly see that any of these coefficients identifies to 1 in the BCS case. With this in mind, let us now give some intuition on how the BCS relation (4) can eventually be seen as a special limit of the PBCS case. Using different recurrence relations, it can be shown that

$$n_i = N|x_i|^2\frac{I_{N-1}}{I_N} - N(N-1)|x_i|^4\frac{I_{N-2}}{I_N} + \cdots + (-1)^{N-1}N!|x_i|^{2N}\frac{I_0}{I_N}.$$

Assuming that all α_K are equal to 1 gives

$$n_i = |x_i|^2\{1 - |x_i|^2 + \cdots + |x_i|^{2(N-1)}\},$$

which identifies with the BCS case, i.e., $n_i = |x_i|^2/(1+|x_i|^2)$ as $N \to \infty$.

[1] P. Ring and P. Schuck, *The Nuclear Many-Body Problem* (Springer-Verlag, Berlin, 1980).
[2] D. M. Brink and R. A. Broglia, *Nuclear Superfluidity: Pairing in Finite Systems* (Cambridge University Press, 2005).
[3] J. von Delft and D. C. Ralph, Phys. Rep. **345**, 61 (2001).
[4] J. Bardeen, L. N. Cooper, and J. R. Schrieffer, Phys. Rev. **108**, 1175 (1957).
[5] R. W. Richardson, J. Math. Phys. **6**, 1034 (1965).
[6] R. W. Richardson, Phys. Rev. **144**, 874 (1966).
[7] R. W. Richardson, Phys. Rev. **141**, 949 (1966).

[8] M. Bender and P.-H. Heenen, Rev. Mod. Phys. **75**, 121 (2003).
[9] J. R. Stone and P.-G. Reinhard, Prog. Part. Nucl. Phys. **58**, 587 (2007).
[10] B. Bayman, Nucl. Phys. **15**, 33 (1960).
[11] T. R. Rodríguez, J. L. Egido, and L. M. Robledo, Phys. Rev. C **72**, 064303 (2005).
[12] M. Anguiano, J. L. Egido, and L. M. Robledo, Nucl. Phys. A **696**, 467 (2001).
[13] J. Dobaczewski, M. V. Stoitsov, W. Nazarewicz, and P.-G. Reinhard, Phys. Rev. C **76**, 054315 (2007).
[14] D. Lacroix, T. Duguet, and M. Bender, Phys. Rev. C **79**, 044318 (2009).
[15] M. Bender, T. Duguet, and D. Lacroix, Phys. Rev. C **79**, 044319 (2009).
[16] T. Duguet, M. Bender, K. Bennaceur, D. Lacroix, and T. Lesinski, Phys. Rev. C **79**, 044320 (2009).
[17] L. M. Robledo, J. Phys. G **37**, 064020 (2010).
[18] T. Duguet and J. Sadoudi, J. Phys. G **37**, 064009 (2010).
[19] D. Lacroix and G. Hupin, Phys. Rev. B **82**, 144509 (2010).
[20] T. L. Gilbert, Phys. Rev. B **12**, 2111 (1975).
[21] P. Hohenberg and W. Kohn, Phys. Rev. **136**, B864 (1964).
[22] N. N. Lathiotakis, S. Sharma, J. K. Dewhurst, F. G. Eich, M. A. L. Marques, and E. K. U. Gross, Phys. Rev. A **79**, 040501(R) (2009).
[23] D. Lacroix, S. Ayik, and P. Chomaz, Prog. Part. Nucl. Phys. **52**, 497 (2004).
[24] J.-A. Sheikh and P. Ring, Nucl. Phys. A **665**, 71 (2000).
[25] D. J. Rowe, T. Song, and H. Chen, Phys. Rev. C **44**, R598 (1991).
[26] D. J. Rowe, Nucl. Phys. A **691**, 691 (2001).
[27] N. Sandulescu and G. Bertsch, Phys. Rev. C **78**, 064318 (2008).
[28] N. Sandulescu, B. Errea, and J. Dukelsky, Phys. Rev. C **80**, 044335 (2009).
[29] A. J. Leggett, *Quantum Liquids* (Oxford University, Oxford, England, 2006), Vol. 1.
[30] E. H. Lieb, Int. J. Quantum Chem. **24**, 243 (1983).
[31] T. Papenbrock and A. Bhattacharyya, Phys. Rev. C **75**, 014304 (2007).
[32] M. G. Bertolli and T. Papenbrock, Phys. Rev. C **78**, 064310 (2008).
[33] G. Csányi and T. A. Arias, Phys. Rev. B **61**, 7348 (2000).
[34] F. Braun and J. von Delft, Phys. Rev. Lett. **81**, 4712 (1998).
[35] M. A. Fernández and J. L. Egido, Phys. Rev. B **68**, 184505 (2003).
[36] M. A. Fernández and J. L. Egido, Eur. Phys. J. B **48**, 305 (2005).
[37] G. Sierra, J. Dukelsky, G. G. Dussel, J. von Delft, and F. Braun, Phys. Rev. B **61**, R11890 (2000).
[38] R. A. Smith and V. Ambegaokar, Phys. Rev. Lett. **77**, 4962 (1996).
[39] M. L. Mehta, *Random Matrices* (Academic Press, 2004).
[40] G. Hupin, D. Lacroix, and M. Bender (unpublished).
[41] I. G. Macdonald, *Symmetric Functions and Hall Polynomials*, 2 (Oxford University, New York, 1999).